

Asymptotic Theory and Sequential Test for General Multi-Armed Bandit Process

Li Yang¹, Xiaodong Yan^{1,*}, Dandan Jiang^{1,*}

¹School of Mathematics and Statistics, Xi'an Jiaotong University, Xi'an 710049, China

*Corresponding authors: yanxiaodong@xjtu.edu.cn; jiangdd@xjtu.edu.cn

Abstract

Multi-armed bandit (MAB) processes constitute a foundational subclass of reinforcement learning problems and represent a central topic in statistical decision theory, but are limited to simultaneous adaptive allocation and sequential test, because of the absence of asymptotic theory under non-i.i.d sequence and sublinear information. To address this open challenge, we propose Urn Bandit (UNB) process to integrate the reinforcement mechanism of urn probabilistic models with MAB principles, ensuring almost sure convergence of resource allocation to optimal arms. We establish the joint functional central limit theorem (FCLT) for consistent estimators of expected rewards under non-i.i.d., non-sub-Gaussian and sublinear reward samples with pairwise correlations across arms. To overcome the limitations of existing methods that focus mainly on cumulative regret, we establish the asymptotic theory along with adaptive allocation that serves powerful sequential test, such as arms comparison, A/B testing, and policy valuation. Simulation studies and real data analysis demonstrate that UNB maintains statistical test performance of equal randomization (ER) design but obtain more average rewards like classical MAB processes.

Keywords: Multi-armed Bandit, Central Limit Theorem, Sequential Test

1 Introduction

In the areas of sequential decision making under uncertainty, such as adaptive experimentation in clinical trials, online testing, and policy evaluation, researchers often need to allocate subjects adaptively while test outcomes sequentially (Zhu and Hu, 2010; Shi et al., 2021). Because Adaptive allocation allows for a more efficient and ethically sound use of resources by preferentially assigning subjects to treatments or arms that perform better (Wei and Durham, 1978; Hu and Rosenberger, 2006; Rosenberger and Lachin, 2016; Wang et al., 2023), while sequential test enables timely inference and early stopping once sufficient evidence has been accumulated (Jennison and Turnbull, 2000; Proschan et al., 2006; Gang et al., 2021; Wang et al., 2024). The integration of adaptive allocation and sequential test is fundamental but challenging for the design of experiments that are efficient and support timely and informed decision-making.

The multi-armed bandit (MAB) framework provides a flexible statistical decision method for adaptive allocation in sequential experiments. By balancing *exploration* and *exploitation* according to historical results, MAB models allocate more resources to better performing arms, enhancing the statistical efficiency and ethicality of adaptive designs (Sutton and Barto, 2018). In recent years, the framework has inspired a rich class of algorithms, including ε -greedy strategies (Sutton and Barto, 2018), upper confidence bound (UCB) methods (Agrawal, 1995; Auer et al., 2002; Audibert et al., 2009; Garivier and Cappé, 2011), and posterior sampling approaches such as Thompson Sampling (Thompson, 1933; Agrawal and Goyal, 2012; Qi et al., 2025). In practical applications such as online advertising and recommendation systems, strategy selections are continuously updated based on observed results, which has motivated numerous extensions of the classical MAB framework by considering more information in the learning procedure for more efficient adaptive allocation, such as selecting multiple arms simultaneously and allowing correlated rewards across arms (Anantharam et al., 1987; Xia et al., 2016; Thananjeyan et al., 2021; Gaharwar et al., 2020; Gupta et al., 2021).

Efficient adaptive allocation often calls for statistically principled sequential test to support effective policy learning, and the statistical foundations of sequential test can be

traced back to the pioneering work of [Wald \(1945\)](#), who introduced the sequential probability ratio test and established its optimality properties. Building on this foundation, [Armitage \(1960\)](#) developed sequential methods adapted to clinical trials, emphasizing practical implementation and ethical considerations. In practical sequential test, the Type I error rate will be inflated due to multiple comparisons, making it necessary to specify rejection boundaries in each interim analysis. For example, [Pocock \(1977\)](#) suggested a group sequential design with equal rejection boundaries in each interim analysis, providing a practical and easily implemented approach to early stopping. [O'Brien and Fleming \(1979\)](#) introduced a multiple testing procedure in which the critical values are highly conservative at early analyses and gradually relax at later stages, improving the statistical efficiency of final inference. Sequentially, [Lan and DeMets \(1983\)](#) proposed the α spending function approach, which allows flexible allocation of the cumulative Type I error across arbitrarily timed interim analyses while maintaining overall error control. More recently, [Jennison and Turnbull \(2000\)](#) provides a comprehensive treatment of group sequential designs, including error control, stopping boundaries, and statistical efficiency comparisons. Building on these theoretical developments, sequential test procedures have also been widely applied beyond clinical trials, including online multiple testing and false discovery rate control ([Gang et al., 2021](#)), online A/B testing ([Ju et al., 2019](#); [Johari et al., 2022](#); [Shi et al., 2023](#); [Yu et al., 2024](#); [Larsen et al., 2024](#)), and sparse recovery ([Wang et al., 2024](#)).

Recent developments in sequential test have increasingly focused on integrating adaptive allocation and sequential test. Specifically, [Zhu and Hu \(2010\)](#) developed a sequential test for two-arm response-adaptive randomized clinical trials under a doubly adaptive biased coin design (DBCD), where the allocation proportion converges to an interior target. This yields arm-specific sample sizes of linear order and leads to a standard Brownian motion limit for the sequential test statistics, which justifies applying classical group sequential boundaries. More recently, [Shi et al. \(2021\)](#) studied sequential test under ε -greedy allocation, inducing history-dependent and typically imbalanced sampling across arms. Since the sequential test statistics do not admit the standard Brownian motion ap-

proximation underlying classical group sequential designs, they calibrated group sequential boundaries via an online bootstrap procedure that estimates the variance-covariance structure of interim statistics. Alternatively, e-values have been adopted for sequential test via the framework of always-valid inference (Johari et al., 2022), which allows continuous test and optional stopping while controlling Type I error. This always-valid perspective has been further extended to adaptive data streams, including contextual bandits, enabling anytime-valid inference under adaptive sampling and optional stopping (Waudby-Smith et al., 2024; Ramdas et al., 2023). This line of work is largely nonasymptotic: validity is obtained by constructing nonnegative supermartingales (e-processes) under null hypothesis and applying Ville’s inequality, yielding time-uniform Type I error control for arbitrary stopping times.

Despite recent advances, the combination of bandit adaptive allocation and sequential test introduces unique challenges. First, bandit adaptive allocation induces complex, history-dependent dynamics in which allocation decisions depend on past outcomes (Mallard and Munos, 2011; Nie et al., 2018). Second, while much of the existing literature focuses on optimizing cumulative regret (Lai and Robbins, 1985; Agrawal and Goyal, 2012; Auer et al., 2002), from a statistical inference perspective, the central issues are the accurate estimation of expected rewards and rigorous quantification of uncertainty. This issue is further amplified when rewards are correlated across arms, since the resulting covariance structure of the estimators becomes nontrivial. Third, sequential test is particularly challenging because bandit allocation can yield highly unbalanced sampling in which some arms receive vanishing sampling proportions. This necessitates online updating of test statistics and a valid characterization of their joint law across interim analyses to control the cumulative Type I error (Zhu and Hu, 2010, 2012).

Motivated by these challenges under sublinear information and non-i.i.d sequence with cross-arm correlations, we develop a Urn Bandit (UNB) process and it integrates the reinforcement mechanism of urn probabilistic models with multi-armed bandit principles by using the multivariate hypergeometric sampling distribution to generate the weight vector of arms selection. For accommodating simultaneous adaptive allocation and se-

quential test, we consider some combinations of expected rewards with a developed UNB process. Specifically, we consider testing hypotheses of the form

$$H_0 : h(\boldsymbol{\mu}_{[\mathcal{A}]}) \in \mathcal{K}_0 \quad \text{versus} \quad H_1 : h(\boldsymbol{\mu}_{[\mathcal{A}]}) \notin \mathcal{K}_0, \quad (1)$$

where $\boldsymbol{\mu} = (\mu_1, \dots, \mu_d)^\top$ denotes the vector of expected rewards, with the subscript $[\mathcal{A}]$ highlighting that the samples are collected under the adaptive allocation rule $\mathcal{A} = \{\mathbf{a}_1, \mathbf{a}_2, \dots, \mathbf{a}_t, \dots\}$. Different choices of the function $h(\cdot)$ accommodate a wide range of practical objectives. Such as $h(\boldsymbol{\mu}_{[\mathcal{A}]}) = \mu_1 - \mu_2$, which corresponds to testing the equality of the two arm means. Table 1 summarizes the key structural differences between existing approaches and our proposed UNB framework. The key contributions are listed as follows:

(i) To overcome the limitations of existing MAB methods that focus mainly on the cumulative regret analysis for adaptive allocation, we develop a unified framework that integrates adaptive allocation and sequential test simultaneously.

(ii) For the methodology, we propose a new and general MAB process termed UNB by generating non-i.i.d., non-sub-Gaussian, and sublinear reward samples with pairwise correlations across arms. UNB integrates the adaptive reinforcement of the probabilistic urn model with the *exploration-exploitation* principle of MAB, implementing a cumulative reward driven multivariate hypergeometric allocation.

(iii) Theoretically, we establish a functional central limit theorem (FCLT) for the expected reward estimator process under adaptive allocation. Since the cumulative sample size of suboptimal arms grows sublinearly, we apply an information time transformation, after which the sequential test statistic converges to standard Brownian motion, justifying the use of classical group sequential boundaries.

The remainder of this paper is organized as follows. In Section 2, we present the urn bandit process for adaptive allocation. Section 3 provides the asymptotic theory and statistical inference. In Section 4, we show the sequential test under the UNB Process. Sections 5 and 6 check the performance of the proposed method by conducting extensive simulation studies and analyzing real data. Section 7 gives some concluding remarks. Proofs of all theoretical results, including lemmas, corollaries, and theorems, are deferred

to the Supplementary Material.

Table 1: Comparison of adaptive designs across key aspects: adaptivity of allocation, dependence across arms, non-sub-Gaussian rewards, sublinear information growth (i.e., sublinear sample size accumulation for suboptimal arms), FCLT for reward estimators, and support for sequential testing.

	Adaptivity Allocation	Dependence across arms	Non-sub Gaussian	Sublinear Information	FCLT	Sequential Test
Zhu and Hu (2010)	✓	✗	✓	✗	✓	✓
May and Flournoy (2009)	✓	✗	✓	✓	✗	✗
Qi et al. (2025)	✓	✗	✗	✓	✗	✗
Gaharwar et al. (2020)	✓	✓	✗	✓	✗	✗
Chen and Lu (2025)	✓	✗	✗	✓	✗	✗
Zhu and Hu (2012)	✓	✗	✓	✗	✓	✓
Shi et al. (2021)	✓	✗	✗	✗	✓	✓
UNB (Ours)	✓	✓	✓	✓	✓	✓

2 Novel Bandit Process and Test Problem

2.1 The UNB Process for Adaptive Allocation

Consider a d -armed bandit problem where an agent sequentially interacts with an environment. The action at each round t is to select a subset of arms to play, denoted by $\mathcal{A}_t \subseteq \{1, 2, \dots, d\}$. Following this action, the environment returns a reward vector $\boldsymbol{\xi}_t$ containing a single reward $\xi_{t,k}$ for each arm $k \in \mathcal{A}_t$.

The agent’s decision making is governed by a novel UNB policy. This policy is characterized by an integer weight vector, $\mathbf{X}_t = (X_{t,1}, \dots, X_{t,d})$, which is adaptively generated based on historical observation. The action set is then formed by the arms that receive a non-zero weight, i.e., $\mathcal{A}_t = \{k : X_{t,k} > 0\}$. Let the history be the σ -field generated by past weights and rewards, $\mathcal{F}_t = \sigma(\{\mathbf{X}_i, \boldsymbol{\xi}_i : 1 \leq i \leq t\})$. The core of the policy is the update rule for the cumulative weighted reward vector \mathbf{R}_t . After observing the rewards $\boldsymbol{\xi}_t$, the memory is updated by

$$\mathbf{R}_t = \mathbf{R}_{t-1} + \mathbf{X}_t \odot \boldsymbol{\xi}_t,$$

where \odot denotes the Hadamard product. This rule ensures that the impact of a reward

is amplified by its corresponding weight. The policy for generating the weight vector \mathbf{X}_t from the memory \mathbf{R}_{t-1} is defined by Multivariate Hypergeometric sampling distribution:

$$\mathbf{X}_t \sim \text{Multi-Hyper}(N_t; \mathbf{R}_{t-1}),$$

where $N_t = \sum_{k=1}^d X_{t,k}$ is the reinforcement budget for the round. This mechanism implements a reinforcement principle: arms with higher cumulative rewards are stochastically assigned larger weights, while ensuring continued exploration for all arms with positive rewards. Algorithm 1 provides a formal description.

Algorithm 1 The UNB Process for Adaptive Allocation

Require: Horizon T , burn in period n_0 , and total reinforcement budget N_t for each round $t \in \{1, 2, \dots, T\}$.

- 1: **Initialization:** Pull each arm n_0 times, observe the rewards for each arm, and compute the initial weighted rewards \mathbf{R}_0 by summing the observed rewards;
 - 2: **for** $t = 1$ to T **do**
 - 3: Generate the weights $\mathbf{X}_t \sim \text{Multi-Hyper}(N_t; \mathbf{R}_{t-1})$;
 - 4: Identify action set $\mathcal{A}_t = \{k : X_{t,k} > 0\}$;
 - 5: Observe outcomes $\{\xi_{t,k} : k \in \mathcal{A}_t\}$ and form the reward vector $\boldsymbol{\xi}_t$;
 - 6: Update cumulative weighted reward: $\mathbf{R}_t \leftarrow \mathbf{R}_{t-1} + \mathbf{X}_t \odot \boldsymbol{\xi}_t$.
 - 7: **end for**
-

We assume the total reinforcement budget $\{N_t, t \geq 1\}$ are random variables that take values in a bounded set of positive integers, and satisfy

$$\mathbb{E}(N_{t+1} | \mathcal{F}_t) \rightarrow N, \quad \text{and} \quad \mathbb{E}(N_{t+1}^2 | \mathcal{F}_t) \rightarrow Q, \quad a.s..$$

For the rewards $\{\boldsymbol{\xi}_t, t \geq 1\}$, we assume that for each arm $k \in \{1, \dots, d\}$,

$$\mu_{k,t} = \mathbb{E}(\xi_{t,k}) \rightarrow \mu_k, \quad \text{and} \quad \sigma_{k,t}^2 = \mathbb{V}\text{ar}(\xi_{t,k}) \rightarrow \sigma_k^2.$$

Furthermore, to accommodate the dependency between arms, we assume that the cross-arm covariance and correlation satisfy

$$C_{ij,t} = \mathbb{C}\text{ov}(\xi_{t,i}, \xi_{t,j}) \rightarrow C_{ij}, \quad \text{and} \quad \rho_{ij,t} = \mathbb{C}\text{orr}(\xi_{t,i}, \xi_{t,j}) \rightarrow \rho_{ij},$$

for any pair of distinct arms i and j . Assumptions on the moments and correlations imply

the non-i.i.d sequences of rewards generated by UNB process.

A bandit algorithm is characterized by its sequential feedback loop, where past outcomes inform future actions. The classical approach uses an unweighted cumulative reward to store the history of outcomes. Our framework generalizes this concept by introducing a cumulative weighted reward vector \mathbf{R}_t , which serves to represent the agent’s belief about the quality of each arm. Through the weighted reinforcement mechanism, $\mathbf{R}_t = \mathbf{R}_{t-1} + \mathbf{X}_t \odot \boldsymbol{\xi}_t$, we provide a more flexible and expressive representation. This mechanism enables our framework to naturally handle both the simultaneous observation of multiple arms and the presence of correlated rewards across them. Ultimately, this enhanced modeling capability leads to more efficient and powerful hypothesis testing in adaptive designs. Table 2 compares the UNB process with classical bandit algorithms in terms of their allocation mechanisms and inferential validity.

To better understand the long-term behavior of the UNB algorithm, we examine how its key quantities evolve over time. We define the normalized cumulative weighted reward vector \mathbf{Z}_n , the cumulative weight $W_{n,k}$ for arm k up to stage n , the sample size $S_{n,k}$ for arm k and the total sample size S_n respectively as

$$\mathbf{Z}_n = \frac{\mathbf{R}_n}{|\mathbf{R}_n|}, \quad W_{n,k} = \sum_{j=1}^n X_{jk}, \quad S_{n,k} = \sum_{j=1}^n \mathbb{I}(X_{jk} > 0), \quad \text{and } S_n = \sum_{k=1}^d S_{n,k}.$$

In addition, let $\mu^* = \max\{\mu_1, \mu_2, \dots, \mu_d\}$ be the largest expected reward of all arms.

Lemma A.1 and A.2 in Appendix A detail the algorithm’s long-term behavior, underpinning subsequent analysis. First, the reinforcement mechanism ensures the algorithm identifies the best-performing arms. As shown in Lemma A.1, the proportion of cumulative weight assigned to the set of optimal arms converges almost surely to 1. Furthermore, the normalized cumulative weighted reward vector \mathbf{Z}_n converges almost surely to a limit vector \mathbf{Z} , where the weights corresponding to suboptimal arms vanish asymptotically, while the weights for optimal arms remain strictly positive. Second, the algorithm maintains sufficient exploration for valid inference. Lemma A.2 establishes that for any suboptimal arm k , the cumulative weight $W_{n,k}$ grows at a sublinear rate of $O_{a.s.}(n^{\mu_k/\mu^*})$,

which implies that the sample size $S_{n,k}$ grows at the same rate. These properties ensure both efficiency in allocation and the conditions for the asymptotic theory that follows.

Table 2: Comparison of the UNB process with classical bandit algorithms, in terms of adaptive allocation rules and the feasibility of statistical inference.

Method	ε -greedy	UCB	UNB (Ours)
Objective	Fixed exploration	Regret minimization	Joint allocation and test
Allocation mechanism	Explore with probability ε	Pull the single arm maximizing an upper confidence index	Subset selection via cumulative weighted rewards
Statistical inference capability	Standard asymptotics can be miscalibrated under adaptivity; valid inference relies on bootstrap or other calibration methods	Inference is feasible under additional regularity conditions (e.g., sub-Gaussian rewards), possibly with further calibration	Native: sequential validity under stated assumptions via FCLT and information fraction transformation

2.2 Hypothesis on Bandit’s Arms

Our primary inferential goal is to test hypotheses concerning some functionals of the expected rewards from the d arms, $\boldsymbol{\mu} = (\mu_1, \mu_2, \dots, \mu_d)^\top$ by adopting the testing framework (1). We highlight two representative instances.

a) **Linear Combinations of Arms.** We consider linear hypotheses of the form:

$$H_0 : \boldsymbol{\beta}^\top \boldsymbol{\mu}_{[A]} \in \mathcal{K}_0 \quad \text{versus} \quad H_1 : \boldsymbol{\beta}^\top \boldsymbol{\mu}_{[A]} \notin \mathcal{K}_0, \quad (2)$$

where \mathcal{K}_0 is a prespecified constraint set, and $\boldsymbol{\beta} \in \mathbb{R}^d$ specifies the contrast of interest. Different choices of $\boldsymbol{\beta}$ and \mathcal{K}_0 recover a broad range of familiar testing problems. Let \mathbf{e}_k denote the k th standard basis vector in \mathbb{R}^d . Specifically:

- *A/B Testing.* Setting $\boldsymbol{\beta} = \mathbf{e}_i - \mathbf{e}_j$ and $\mathcal{K}_0 = (-\infty, 0]$ yields $H_0 : \mu_i - \mu_j \leq 0$, representing typical A/B testing (Johari et al., 2017; Zhang et al., 2025).

- *Benchmarking against a Threshold.* Choosing $\boldsymbol{\beta} = \mathbf{e}_k$ and $\mathcal{K}_0 = (-\infty, K_0]$ reduces the problem to assessing whether the expected reward of a single arm does not exceed a fixed benchmark K_0 (Locatelli et al., 2016; Kano et al., 2019).

- *Comparison with Control Group Average.* More structured comparisons, such as evaluating a new arm against the average of multiple controls, are obtained by contrasts such as $\boldsymbol{\beta} = (1, -0.5, -0.5, 0, \dots, 0)^\top$, typically with $\mathcal{K}_0 = (-\infty, 0]$.

- *General Weighted Objectives.* The framework (2) also covers general inference on

weighted means by taking $\beta = \mathbf{w}$ for any prespecified weight vector \mathbf{w} .

b) Nonlinear Functionals of Arms. Beyond linear contrasts, the framework also accommodates smooth nonlinear functionals of $\boldsymbol{\mu}$. Let $h : \mathbb{R}^d \rightarrow \mathbb{R}$ be continuously differentiable and consider

$$H_0 : h(\boldsymbol{\mu}_{[\mathcal{A}]}) \leq 0 \quad \text{versus} \quad H_1 : h(\boldsymbol{\mu}_{[\mathcal{A}]}) > 0, \quad (3)$$

A representative example is inference for relative effects, for instance $h(\boldsymbol{\mu}_{[\mathcal{A}]}) = \mu_i/\mu_j$, which corresponds to lift-type effect measures commonly reported in online controlled experiments (Larsen et al., 2024). Under the stated smoothness condition on h (in particular, $\mu_j > 0$), inference for (3) follows from the limit theory for linear functionals together with the Delta method.

While these problems are standard under static designs, UNB changes the inferential context by generating adaptive, history-dependent data. Such integration is attractive in multi-arm experiments where both ethical considerations and statistical efficiency favor making timely decisions.

3 Asymptotic Theory and Statistical Inference

This section establishes the asymptotic theory under the UNB allocation and constructs the testing statistic for the testing problem (1), then analyze its asymptotic power properties. To facilitate these derivations, we impose the following assumptions on the reward process.

Assumption 1. *There exists a constant C such that $\sup_{n,k} \mathbb{E}(\xi_{nk}^3) < C$.*

Assumption 2. *For all $k \in \{1, 2, \dots, d\}$, $|\mu_{k,n} - \mu_k| = o(n^{-\frac{\mu_k}{2\mu^*}})$.*

Assumption 1 requires only uniformly bounded third moments. Unlike bandit methods that rely on sub-Gaussian tail assumptions to obtain finite sample concentration guaranties, our asymptotic analysis framework remains valid for a broader class of reward distributions, including those that are not sub-Gaussian, e.g., Poisson or expo-

nential rewards. The Assumption 2 relaxes the classical condition of time-homogeneous expected rewards and accommodates environments with drifting expected rewards, where the means are allowed to vary over time but converge at a sufficiently fast rate so that the induced bias is asymptotically negligible.

3.1 Joint Asymptotic Distribution of the Mean Estimators

For each arm k , the natural estimator for the unknown expected reward μ_k is the weighted sample mean of the observed responses:

$$\hat{\mu}_{k,n} = \frac{\sum_{t=1}^n X_{t,k} \xi_{t,k}}{\sum_{t=1}^n X_{t,k}}.$$

Under the UNB allocation, both the sampling indicators $X_{t,k}$ and the effective sample sizes are random and history dependent. Consequently, the limiting behavior of the estimators is governed by the complex interplay of adaptive allocation, subset selection, and cross-arm dependence. The following theorem rigorously establishes the joint CLT for $(\hat{\mu}_{1,n}, \dots, \hat{\mu}_{d,n})^\top$ and explicitly characterizes the asymptotic covariance structure.

Theorem 3.1. *Under Assumptions 1–2, the estimators of the expected rewards are asymptotically normally distributed, and satisfy that*

$$\hat{\Sigma}_n^{-1/2} \begin{pmatrix} \sqrt{W_{n,1}}(\hat{\mu}_{1,n} - \mu_1) \\ \sqrt{W_{n,2}}(\hat{\mu}_{2,n} - \mu_2) \\ \vdots \\ \sqrt{W_{n,d}}(\hat{\mu}_{d,n} - \mu_d) \end{pmatrix} \xrightarrow{L} \mathcal{N}(\mathbf{0}, \mathbf{I}),$$

and the estimated covariance matrix $\hat{\Sigma}_n$ is defined element-wise by:

$$[\hat{\Sigma}_n]_{pq} = \begin{cases} \hat{\sigma}_{p,n}^2 \left[\hat{Z}_{p,n} \left(\frac{\hat{m}_{Q,n}}{\hat{m}_{N,n}} - 1 \right) + 1 \right], & \text{for } p = q, \\ \hat{C}_{pq,n} \sqrt{\hat{Z}_{p,n} \hat{Z}_{q,n}} \left(\frac{\hat{m}_{Q,n}}{\hat{m}_{N,n}} - 1 \right), & \text{for } p \neq q. \end{cases} \quad (4)$$

Here $\hat{\sigma}_{p,n}^2$ is a consistent estimator of σ_p^2 , and $\hat{C}_{pq,n}$ is a consistent estimator of the cross-

arm covariance C_{pq} . The quantity $\hat{Z}_{p,n}$ estimates the limiting allocation proportion Z_p , and $\hat{m}_{N,n}$ and $\hat{m}_{Q,n}$ estimate the limiting first and second conditional moments of the reinforcement budget, defined by

$$m_N = \lim_{n \rightarrow \infty} \mathbb{E}(N_n | \mathcal{F}_{n-1}), \quad \text{and} \quad m_Q = \lim_{n \rightarrow \infty} \mathbb{E}(N_n^2 | \mathcal{F}_{n-1}).$$

Explicit expressions for these plug-in estimators are provided in Appendix A. Notably, $\hat{\Sigma}_n$ in (4) captures the additional variance and cross-arm correlations induced by the adaptive design, which are absent in fixed-design settings.

3.2 Construction of the Test Statistics

To facilitate the subsequent asymptotic analysis concerning smooth functionals of the expected rewards (1), particularly regarding the convergence rates of the test statistic, we introduce the following notation to characterize the subset of arms involved in the hypothesis. Let \mathcal{T}_h denote the set of indices $k \in \{1, 2, \dots, d\}$ on which $h(\cdot)$ depends. Accordingly, we define

$$\mu_{h,\min} = \min\{\mu_k : k \in \mathcal{T}_h\}, \quad \text{and} \quad \mathcal{T}_{h,\min} = \{k : \mu_k = \mu_{h,\min}, k \in \mathcal{T}_h\}.$$

For asymptotic analysis, we assume h satisfies the following properties.

Assumption 3. *The function $h : \mathbb{R}^d \rightarrow \mathbb{R}$ is continuously differentiable in a neighborhood of $\boldsymbol{\mu}$. Furthermore, there exists $k \in \mathcal{T}_{h,\min}$ such that $\frac{\partial h(\boldsymbol{\mu})}{\partial \mu_k} \neq 0$.*

Applying the multivariate Delta method to Theorem 3.1 yields a valid asymptotic distribution that explicitly accounts for the adaptive covariance structure.

Theorem 3.2. *Under Assumptions 1–3, it holds that*

$$\frac{h(\hat{\boldsymbol{\mu}}_n) - h(\boldsymbol{\mu})}{\hat{\sigma}_{h,n}} \xrightarrow{L} \mathcal{N}(0, 1),$$

where the consistent variance estimator $\hat{\sigma}_{h,n}^2$ is given by the quadratic form

$$\hat{\sigma}_{h,n}^2 = \sum_{i=1}^d \sum_{j=1}^d \frac{\partial_i h(\hat{\boldsymbol{\mu}}_n) \partial_j h(\hat{\boldsymbol{\mu}}_n)}{\sqrt{W_{n,i} W_{n,j}}} [\hat{\boldsymbol{\Sigma}}_n]_{ij}.$$

Here, $\partial_k h(\cdot)$ denotes the partial derivative of h with respect to its k th argument μ_k , and $\partial_k h(\hat{\boldsymbol{\mu}}_n)$ represents this derivative evaluated at the consistent estimator $\hat{\boldsymbol{\mu}}_n$.

For example, the one-sided test statistic for hypothesis $H_0 : h(\boldsymbol{\mu}_{[A]}) \leq 0$ is

$$\Psi_n = \frac{h(\hat{\boldsymbol{\mu}}_n)}{\hat{\sigma}_{h,n}}. \quad (5)$$

Under the null hypothesis boundary, Theorem 3.2 implies $\Psi_n \xrightarrow{L} \mathcal{N}(0, 1)$. Therefore, for a test with a significance level α , the rejection region is given by $\mathcal{C}_\alpha = \{\Psi_n > z_\alpha\}$, where z_α is the upper α -quantile of the standard normal distribution $\mathcal{N}(0, 1)$. To understand the structural difference between our adaptive test and a classical fixed-design test, we examine the variance estimator $\hat{\sigma}_{h,n}^2$. It can be factored as

$$\hat{\sigma}_{h,n}^2 = \hat{\Gamma}_n \cdot \hat{\Lambda}_n \cdot \left(\sum_{k=1}^d \frac{(\partial_k h(\hat{\boldsymbol{\mu}}_n))^2 \hat{\sigma}_{k,n}^2}{S_{n,k}} \right),$$

with

$$\hat{\Gamma}_n = \frac{\sum_{i,j} \frac{\partial_i h(\hat{\boldsymbol{\mu}}_n) \partial_j h(\hat{\boldsymbol{\mu}}_n)}{\sqrt{W_{n,i} W_{n,j}}} [\hat{\boldsymbol{\Sigma}}_n]_{ij}}{\sum_{k=1}^d \frac{(\partial_k h(\hat{\boldsymbol{\mu}}_n))^2 \hat{\sigma}_{k,n}^2}{W_{n,k}}} \quad \text{and} \quad \hat{\Lambda}_n = \frac{\sum_{k=1}^d \frac{(\partial_k h(\hat{\boldsymbol{\mu}}_n))^2 \hat{\sigma}_{k,n}^2}{W_{n,k}}}{\sum_{k=1}^d \frac{(\partial_k h(\hat{\boldsymbol{\mu}}_n))^2 \hat{\sigma}_{k,n}^2}{S_{n,k}}}.$$

The term $\sum_{k=1}^d \frac{(\partial_k h(\hat{\boldsymbol{\mu}}_n))^2 \hat{\sigma}_{k,n}^2}{S_{n,k}}$ is the classical variance component. The term $\hat{\Gamma}_n$ is the adaptive reinforcement factor, and the term $\hat{\Lambda}_n$ is the weight-sample discrepancy factor. Let $\mathcal{I} = \{k : \mu_k = \mu^*\}$ denote the set of optimal arms. The following lemma shows the asymptotic behavior of the $\hat{\Gamma}_n$.

Lemma 3.3. *Suppose Assumptions 1–3 hold. If there exists $k \notin \mathcal{I}$ such that $\partial_k h(\boldsymbol{\mu}) \neq 0$, then $\lim_{n \rightarrow \infty} \hat{\Gamma}_n = 1$. Otherwise, if $\partial_k h(\boldsymbol{\mu}) = 0$ for all $k \notin \mathcal{I}$, then*

$$\hat{\Gamma}_{n \rightarrow \Gamma} = 1 + \left(\frac{Q}{N} - 1 \right) \frac{\sum_{i,j \in \mathcal{I}} \partial_i h(\boldsymbol{\mu}) \partial_j h(\boldsymbol{\mu}) C_{ij}}{\sum_{k \in \mathcal{I}} (\partial_k h(\boldsymbol{\mu}))^2 \sigma_k^2 / Z_k}, \quad \text{a.s., as } n \rightarrow \infty. \quad (6)$$

Lemma 3.3 reveals that the variance inflation in (6) emerges from two distinct mechanisms when the tested functional involves only optimal arms. The first is a subset selection effect, captured by the factor $(Q/N - 1)$, which reflects the impact of batch sampling on the effective reinforcement of adaptively selected arms and vanishes only in the single-play regime ($N_t \equiv 1$). The second is a structural interaction effect, arising from the joint influence of the functional gradient $\partial h(\boldsymbol{\mu})$, the cross-arm dependence structure encoded in C_{ij} , and the limiting allocation proportions Z_k . Together, these components characterize how adaptive batching modifies the variance structure relative to classical fixed-design settings.

When $N_t \equiv 1$, the proposed test statistic reduces to the classical form applied to random sample sizes. In contrast, for $N_t > 1$, ignoring the adaptive variance correction leads to substantial size distortion. Figure 1 illustrates this effect in a two-arm setting under $H_0 : \mu_1 = \mu_2$. The naive classical test fails to control the nominal size, whereas the proposed statistic Ψ_n achieves accurate size control irrespective of the presence of cross-arm correlation.

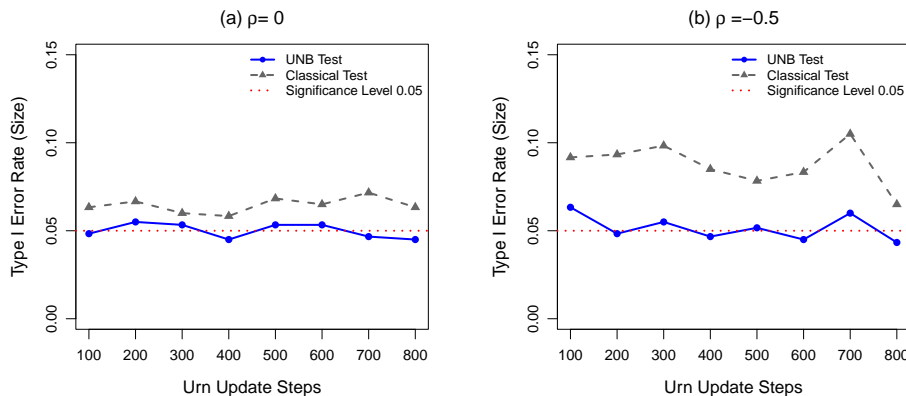


Figure 1: Simulation Type I error rate (Size) of the UNB test and the naive classical test under the null hypothesis $H_0 : \mu_1 = \mu_2$ with a fixed batch size of $N_t = 4$ across different cross-arm dependence. UNB test maintains the Type I error rate.

3.3 Asymptotic Power Analysis

This section turns to explore the asymptotic behavior under fixed alternatives and characterizes the asymptotic power of the test. Notably, the divergence rate of the test statistic

is governed by $\mu_{h,\min}/\mu^*$, indicating that the test’s asymptotic efficiency is constrained by the arm with the minimum effective sample size.

Theorem 3.4. *Suppose Assumptions 1–3 hold. Under any fixed alternative $H_1 : h(\boldsymbol{\mu}_{[A]}) = \tau > 0$, conditional on the limiting scaled allocation proportions of the arms, the distribution of Ψ_n is asymptotically normal with unit variance and a mean that diverges at a rate of $n^{\frac{\mu_{h,\min}}{2\mu^*}}$. Thus, the power of the test converges to 1 as $n \rightarrow \infty$. That is,*

$$\mathbb{P}_{H_1}(\text{Reject } H_0) = \mathbb{P}_{H_1}(\Psi_n > z_\alpha) \rightarrow 1, \quad \text{as } n \rightarrow \infty.$$

To contextualize the asymptotic statistical efficiency of the UNB test, we compare it with two widely used allocation benchmarks: equal randomization (ER) and the UCB algorithm. ER is a non-adaptive benchmark that maximizes power, and the UCB represents a strategy optimized for regret minimization.

A principled comparison requires evaluating each strategy as a holistic data-generating process. In adaptive settings, the sample sizes are endogenously determined by the allocation rule, whereby inference efficiency is intrinsically tied to the allocation mechanism. Our comparison therefore follows three principles: (i) each strategy generates its own observation sequence; (ii) each is evaluated using its theoretically valid test statistic to ensure Type I error control; and (iii) all strategies operate under identical settings and constraints, specifically a fixed sample budget and a nominal level of $\alpha = 0.05$. For UNB, we use the statistic Ψ_n defined in (5). For ER, the classical Z -statistic Ψ_n^{ER} is used. For UCB, we adopt a Z -type studentized statistic based on the pull counts $T_{n,k}$ and the corresponding sample mean and variance estimators. This choice is motivated by recent asymptotic normality results for UCB based mean estimators under sub-Gaussian reward assumptions; see, e.g., [Khamaru and Zhang \(2024\)](#). Such calibrations may not be guaranteed beyond the sub-Gaussian setting. For completeness, Table 3 summarizes the explicit forms of the test statistics for the UNB, UCB, and ER algorithms across several common hypothesis testing scenarios in Section 2.2.

The correction factors $\hat{\Gamma}_n^{(j)}$, representing the combined effect of $\hat{\Gamma}_n \hat{\Lambda}_n$ under indepen-

Table 3: Summary of test statistics applied by allocation strategies UNB, UCB, ER to hypothesis tests outlined in Section 2.2.

Hypothesis Test	UNB (Ψ_n)	UCB (Ψ_n^{UCB})	ER (Ψ_n^{ER})
$H_0^{(1)} : \mu_1 \leq \mu_2$	$\frac{\hat{\mu}_{1,n} - \hat{\mu}_{2,n}}{\sqrt{\hat{\Gamma}_n^{(1)}} \sqrt{\frac{\hat{\sigma}_{1,n}^2}{S_{n,1}} + \frac{\hat{\sigma}_{2,n}^2}{S_{n,2}}}}$	$\frac{\hat{\mu}_{1,n} - \hat{\mu}_{2,n}}{\sqrt{\frac{\hat{\sigma}_{1,n}^2}{T_{n,1}} + \frac{\hat{\sigma}_{2,n}^2}{T_{n,2}}}}$	$\frac{\bar{\mu}_{1,n} - \bar{\mu}_{2,n}}{\sqrt{\frac{2\hat{\sigma}_{1,n}^2}{n} + \frac{2\hat{\sigma}_{2,n}^2}{n}}}$
$H_0^{(2)} : \mu_k \leq K_0$	$\frac{\hat{\mu}_{k,n} - K_0}{\sqrt{\hat{\Gamma}_n^{(2)}} \sqrt{\frac{\hat{\sigma}_{k,n}^2}{S_{n,k}}}}$	$\frac{\hat{\mu}_{k,n} - K_0}{\sqrt{\frac{\hat{\sigma}_{k,n}^2}{T_{n,k}}}}$	$\frac{\bar{\mu}_{k,n} - K_0}{\sqrt{\frac{\hat{\sigma}_{k,n}^2}{n_k}}}$
$H_0^{(3)} : \mu_1 \leq \frac{\mu_2 + \mu_3}{2}$	$\frac{\hat{\mu}_{1,n} - 0.5(\hat{\mu}_{2,n} + \hat{\mu}_{3,n})}{\sqrt{\hat{\Gamma}_n^{(3)}} \sqrt{\frac{\hat{\sigma}_{1,n}^2}{S_{n,1}} + \frac{0.25\hat{\sigma}_{2,n}^2}{S_{n,2}} + \frac{0.25\hat{\sigma}_{3,n}^2}{S_{n,3}}}}$	$\frac{\hat{\mu}_{1,n} - 0.5(\hat{\mu}_{2,n} + \hat{\mu}_{3,n})}{\sqrt{\frac{\hat{\sigma}_{1,n}^2}{T_{n,1}} + \frac{0.25\hat{\sigma}_{2,n}^2}{T_{n,2}} + \frac{0.25\hat{\sigma}_{3,n}^2}{T_{n,3}}}}$	$\frac{\bar{\mu}_{1,n} - 0.5(\bar{\mu}_{2,n} + \bar{\mu}_{3,n})}{\sqrt{\frac{3\hat{\sigma}_{1,n}^2}{n} + \frac{0.75\hat{\sigma}_{2,n}^2}{n} + \frac{0.75\hat{\sigma}_{3,n}^2}{n}}}$

dence, are defined below. Let $A_{k,n} = \hat{Z}_{k,n} \left(\frac{\hat{m}_{Q,n}}{\hat{m}_{N,n}} - 1 \right) + 1$ denote the arm-specific variance inflation component. Then

$$\hat{\Gamma}_n^{(1)} = \frac{\frac{A_{1,n}\hat{\sigma}_{1,n}^2}{W_{n,1}} + \frac{A_{2,n}\hat{\sigma}_{2,n}^2}{W_{n,2}}}{\frac{\hat{\sigma}_{1,n}^2}{S_{n,1}} + \frac{\hat{\sigma}_{2,n}^2}{S_{n,2}}}, \quad \hat{\Gamma}_n^{(2)} = \frac{A_{k,n}S_{n,k}}{W_{n,k}}, \quad \hat{\Gamma}_n^{(3)} = \frac{\frac{A_{1,n}\hat{\sigma}_{1,n}^2}{W_{n,1}} + \frac{A_{2,n}\hat{\sigma}_{2,n}^2}{4W_{n,2}} + \frac{A_{3,n}\hat{\sigma}_{3,n}^2}{4W_{n,3}}}{\frac{\hat{\sigma}_{1,n}^2}{S_{n,1}} + \frac{\hat{\sigma}_{2,n}^2}{4S_{n,2}} + \frac{\hat{\sigma}_{3,n}^2}{4S_{n,3}}}.$$

With the explicit forms of the test statistics established, we now proceed to a theoretical comparison of their asymptotic powers. While the proposed framework applies to general hypotheses, the fundamental statistical efficiency gap between the strategies is most clearly illuminated in a direct pairwise comparison. Next, we focus our asymptotic analysis on the classical two-arm setup involving a suboptimal arm:

$$H_0 : \mu_1 \leq \mu_2 \quad \text{versus} \quad H_1 : \mu_1 - \mu_2 = \Delta > 0. \quad (7)$$

Under the alternative H_1 in (7), the test statistics satisfy $\Psi_n^{(\cdot)} \stackrel{d}{\approx} \mathcal{N}(\text{NCP}_n^{(\cdot)}, 1)$. The key differentiator is the non-centrality parameter (NCP) induced by each allocation strategy. For the ER benchmark that maximizes power, the NCP scales at the optimal rate of $\text{NCP}_n^{\text{ER}} \asymp \sqrt{n}$. For the adaptive strategies, we have

$$\text{NCP}_n^{\text{UNB}} = \frac{1}{\sqrt{\hat{\Gamma}_n^{(1)}}} \frac{\Delta}{\sqrt{\frac{\hat{\sigma}_{1,n}^2}{S_{n,1}} + \frac{\hat{\sigma}_{2,n}^2}{S_{n,2}}}}, \quad \text{NCP}_n^{\text{UCB}} = \frac{\Delta}{\sqrt{\frac{\hat{\sigma}_{1,n}^2}{T_{n,1}} + \frac{\hat{\sigma}_{2,n}^2}{T_{n,2}}}}. \quad (8)$$

By characterizing the asymptotic growth of the effective sample sizes under each allocation rule, we establish the divergence rates of $\text{NCP}_n^{(\cdot)}$.

Corollary 3.5. *Suppose Assumptions 1–3 hold. In addition, assume that the rewards are sub-Gaussian. Under the fixed alternative $H_1 : \mu_1 - \mu_2 = \Delta > 0$, the $NCP_n^{(\cdot)}$ defined in (8) satisfies that*

$$NCP_n^{\text{UNB}} \asymp \sqrt{n^{\mu_2/\mu^*}}, \quad NCP_n^{\text{UCB}} \asymp \sqrt{\log n}, \quad a.s..$$

Since the asymptotic power is increasing in $NCP_n^{(\cdot)}$, it follows that for sufficiently large n ,

$$\text{Power}^{\text{UNB}} > \text{Power}^{\text{UCB}}.$$

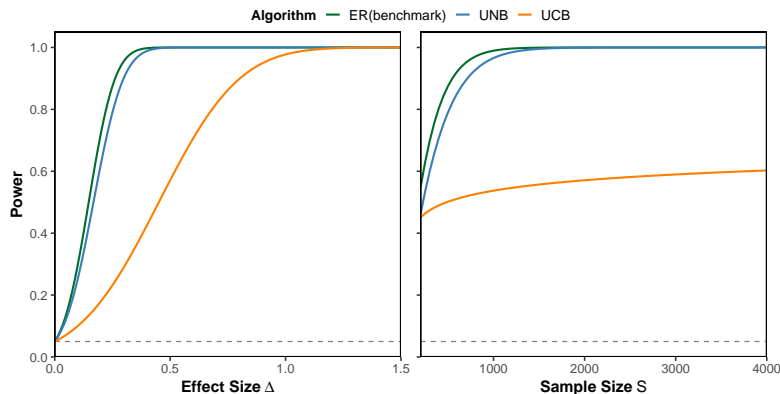


Figure 2: Asymptotic power curves of different allocation strategies for the two-arm test (7) across different difference of arms' expected reward Δ with $S = 2000$ and different sample size S at $\Delta = 0.5$. UNB closely approximates the ER benchmark which maximizes power in both cases.

Corollary 3.5 highlights a fundamental distinction in asymptotic statistical efficiency mechanisms. Comparing the rates with the optimal benchmark $NCP_n^{\text{ER}} \asymp \sqrt{n}$, we observe that UNB preserves a polynomial divergence rate, whereas UCB suffers from a logarithmic rate. This captures the trade-off in adaptive experimentation: more aggressive concentration can reduce inferior arm exposure, but it may also limit the information available for the contrast of interest. To demonstrate these asymptotic behaviors, Figure 2 illustrates the asymptotic power functions of the three strategies against the effect size Δ . As shown, the power curve of UNB closely tracks that of the ER benchmark that maximized power, whereas UCB lags behind due to its logarithmic convergence rate. The following numerical simulation studies also evaluate the similar allocation efficiency and

testing performance of these algorithms. The similar theoretical results for arms' reward analysis can be extended directly to other testing problems in Table 3.

4 Sequential test under the UNB Process

Embedding UNB within a sequential test framework enables learning and early decision-making to be carried out simultaneously, allowing the system to both exploit superior arms and terminate once sufficient evidence against H_0 has accumulated. However, (i) Repeated interim analyses require explicit control of the dependence among interim statistics in order to maintain the nominal Type I error (Armitage et al., 1969); (ii) Classical sequential test typically assume Gaussian approximation with independent increments on a variance-stabilized scale (Jennison and Turnbull, 2000). Yet, UNB exhibits stochastic and heterogeneous variance accumulation: optimal arms grow linearly while suboptimal arms scale sublinearly. This path-dependent non-uniformity obscures appropriate scaling and precludes direct calendar-time boundaries.

4.1 Functional Central Limit Theorem for the UNB Process

We extend fixed-time asymptotics to a FCLT for the vector of weighted mean estimators generated by the UNB process. A key feature is the heterogeneous accumulation of effective sample size across arms: $W_{n,k} = O_{a.s.}(n)$ for optimal arms, whereas $W_{n,k} = O_{a.s.}(n^{\mu_k/\mu^*})$ for suboptimal arms. We show that the normalized estimation error process converges weakly to a continuous Gaussian limit with an explicit covariance structure.

Theorem 4.1 (FCLT with Stable Convergence). *Suppose Assumptions 1–3 hold. Define the weighted cumulative deviation process scaled by the total allocation:*

$$\mathbf{M}_n(t) = \left(\frac{W_{[nt],1}}{\sqrt{W_{n,1}}}(\hat{\mu}_{1,[nt]} - \mu_1), \dots, \frac{W_{[nt],d}}{\sqrt{W_{n,d}}}(\hat{\mu}_{d,[nt]} - \mu_d) \right)^\top, \quad t \in [0, 1].$$

As $n \rightarrow \infty$, the process converges stably in the Skorokhod space $\mathcal{D}([0, 1], \mathbb{R}^d)$:

$$\mathbf{M}_n(\cdot) \xrightarrow{L} \mathbf{G}(\cdot), \quad \text{stably,}$$

where the conditional covariance structure of $\mathbf{G}(\cdot)$ admits the representation:

$$\mathbb{C}ov(\mathbf{G}(t) \mid \mathcal{F}_\infty) = \mathbf{D}(t) \mathbf{V} \mathbf{D}(t),$$

with the time-scaling matrix $\mathbf{D}(t) = \text{diag}(t^{\frac{\mu_1}{2\mu^*}}, \dots, t^{\frac{\mu_d}{2\mu^*}})$ and the asymptotic variance kernel \mathbf{V} defined element-wise by:

$$[\mathbf{V}]_{pq} = \begin{cases} \sigma_p^2 [Z_p (\frac{Q}{N} - 1) + 1], & \text{for } p = q, \\ C_{pq} \sqrt{Z_p Z_q} (\frac{Q}{N} - 1), & \text{for } p \neq q, \end{cases}$$

where Z_k is the almost sure limiting allocation proportion of arm k under UNB.

The diagonal matrix $\mathbf{D}(t)$ formalizes the impact of heterogeneous sampling rates on the fluctuation process. For optimal arms, the exponent $1/2$ recovers the canonical \sqrt{t} scaling of standard Brownian motion, while for suboptimal arms, the smaller exponent $\mu_k/(2\mu^*) < 1/2$ compresses their effective time-scale, dampening variance accumulation relative to the optimal arms.

The convergence in Theorem 4.1 is defined via stable convergence (Rényi, 1963; Hall and Heyde, 1980), because the limiting Gaussian process $\mathbf{G}(\cdot)$ has a random covariance structure driven by \mathcal{F}_∞ -measurable randomness from the adaptive sampling, including the asymptotic allocation proportions \mathbf{Z} . Stable convergence ensures joint convergence with respect to \mathcal{F}_∞ , and is crucial for inference procedures involving random normalization based on data-driven variance estimators.

4.2 Information Fraction Transformation and Canonical Joint Distribution

To ensure valid sequential inference under heterogeneous and sublinear growth n^{μ_k/μ^*} , we adopt the information fraction framework (Jennison and Turnbull, 2000, Chapter 7) resulting sequential test statistic admits a standard Brownian motion limit through indexing analyses by accumulated observed information, i.e., the inverse variance of the

adaptive estimator (Lan et al., 1994; Proschan et al., 2024). Specifically, let $\mathcal{I}_0 = 0$ and $\mathcal{I}_n = (\hat{\sigma}_{h,n}^2)^{-1}$ for $n \geq 1$ denote the observed information for $h(\hat{\boldsymbol{\mu}}_n)$. This choice is natural; defining information as the inverse variance links information directly to precision, implying that a larger \mathcal{I}_n corresponds to a smaller variance and hence a more precise estimate of $h(\boldsymbol{\mu})$ (Lan and Zucker, 1993).

For asymptotic analysis, we index the test process on $[0, 1]$ by the calendar time fraction r and define the information fraction relative to the realized terminal level

$$t_n(r) = \frac{\mathcal{I}_{\lfloor nr \rfloor}}{\mathcal{I}_n}.$$

This yields $t_n(0) = 0$ and $t_n(1) = 1$. Recall $\mu_{h,\min} = \min\{\mu_k : k \in \mathcal{T}_h\}$ and define

$$\gamma = \frac{\mu_{h,\min}}{\mu^*}.$$

The following lemma characterizes the asymptotic scaling of the information fraction for the testing problem (1) relative to the calendar time fraction under UNB.

Lemma 4.2. *Suppose Assumptions 1–3 hold. For any calendar time $0 \leq r < s \leq 1$,*

$$\frac{t_n(r)}{t_n(s)} \xrightarrow{a.s.} \left(\frac{r}{s}\right)^\gamma, \quad \text{as } n \rightarrow \infty. \quad (9)$$

Lemma 4.2 implies a regular-variation type relationship between information fraction and the calendar time fraction. Applying (9) with $s = 1$ and $t_n(1) \equiv 1$, we obtain $t_n(r) \xrightarrow{a.s.} r^\gamma$ for each fixed $r \in [0, 1]$. Hence, the limit $t(r) = r^\gamma$ is strictly increasing on $[0, 1]$ and admits the inverse mapping $g(t) = t^{\frac{1}{\gamma}}$. This motivates reparametrizing the test process to recover the canonical Brownian covariance structure. Utilizing the inverse mapping to identify the calendar time corresponding to the information fraction t , we define the information fraction indexed process $B_n(t)$ for $t \in [0, 1]$ as $B_n(0) = 0$ and

$$B_n(t) = \sqrt{t} \frac{h(\hat{\boldsymbol{\mu}}_{\lfloor ng(t) \rfloor}) - h(\boldsymbol{\mu})}{\hat{\sigma}_{h, \lfloor ng(t) \rfloor}}, \quad \text{for } t \in (0, 1].$$

The reparametrization above is designed to restore the canonical covariance structure required by group sequential theory.

Theorem 4.3 (FCLT under information fraction). *Suppose Assumptions 1–3 hold. As $n \rightarrow \infty$, the process $B_n(\cdot)$ satisfies that*

$$B_n(\cdot) \xrightarrow{L} \mathbb{W}(\cdot),$$

in $\mathcal{D}([0, 1])$, where $\mathbb{W}(\cdot)$ is a standard Brownian motion.

While Theorem 4.3 establishes the asymptotic behavior on the information fraction t , practical interim test is conducted on the calendar time fraction r . To operationalize the testing procedure, we define the sequential statistic process indexed by $r \in (0, 1]$ as

$$\Psi_n(r) = \frac{h(\hat{\boldsymbol{\mu}}_{\lfloor nr \rfloor})}{\hat{\sigma}_{h, \lfloor nr \rfloor}}.$$

The Brownian motion limit in Theorem 4.3 immediately yields the joint distribution of the standardized statistics at any finite collection of information fractions. In particular, under the null hypothesis boundary $h(\boldsymbol{\mu}_{[\mathcal{A}]}) = 0$, evaluating $B_n(\cdot)$ at t_1, \dots, t_K and using $\Psi_n(g(t)) = \frac{B_n(t)}{\sqrt{t}}$ gives the following corollary.

Corollary 4.4. *Suppose Assumptions 1–3 hold. Let $0 < t_1 < t_2 < \dots < t_K \leq 1$ be a fixed sequence of information fractions. Under the null hypothesis boundary $h(\boldsymbol{\mu}_{[\mathcal{A}]}) = 0$, as $n \rightarrow \infty$, the sequential test statistic*

$$(\Psi_n(g(t_1)), \Psi_n(g(t_2)), \dots, \Psi_n(g(t_K)))^\top$$

converges in distribution to a multivariate standard normal vector $(Z_1, \dots, Z_K)^\top$ with mean zero and the covariance structure:

$$\text{Cov}(Z_i, Z_j) = \sqrt{t_i/t_j}, \quad \text{for } i \leq j.$$

The sequential test statistic $(\Psi_n(g(t_1)), \Psi_n(g(t_2)), \dots, \Psi_n(g(t_K)))$ has the asymptot-

ically *canonical joint distribution* defined in (Jennison and Turnbull, 2000, Chapter 3). This result embeds the UNB process in the standard group sequential framework and provides the theoretical basis for using the α spending approach (Lan and DeMets, 1983) to construct stopping boundaries.

Let (c_1, \dots, c_K) denote a sequence of one-sided rejection boundaries. The following corollary shows the asymptotic power of the sequential test.

Corollary 4.5. *Suppose Assumptions 1–3 hold. Under the fixed alternative hypothesis $H_1 : h(\boldsymbol{\mu}_{[A]}) = \tau > 0$, the power of the sequential test converges to 1 as $n \rightarrow \infty$. Formally,*

$$\mathbb{P}_{H_1}(\text{Reject } H_0) = \mathbb{P}_{H_1}(\exists k \leq K : \Psi_n(g(t_k)) > c_k) \rightarrow 1.$$

4.3 Information Planning and Boundary Construction

Sequential test procedure requires two design components: (i) Information planning, which specifies the target information level \mathcal{I}_{\max} to attain the desired power $1 - \eta$ at the prescribed significance level α ; (ii) Stopping boundary construction, which derives a sequence of critical values via an α spending rule to control the overall Type I error. Following Lan and Zucker (1993), we adopt a normal working model for the standardized statistic in (5) and calibrate \mathcal{I}_{\max} accordingly, yielding

$$\mathcal{I}_{\max} = \left(\frac{z_\alpha + z_\eta}{\Delta} \right)^2.$$

To account for repeated interim analyses, we inflate the target information to $\tilde{\mathcal{I}}_{\max} = L\mathcal{I}_{\max}$, where $L > 1$ is set by the number of looks K and the α spending rule (Jennison and Turnbull, 2000, Chapter 3). Interim analyses occur as observed information first exceeds pre-specified fractions of $\tilde{\mathcal{I}}_{\max}$.

To control the overall Type I error at level α , we fix a non-decreasing α spending function $\alpha^* : [0, 1] \rightarrow [0, \alpha]$ with $\alpha^*(0) = 0$ and $\alpha^*(1) = \alpha$. At the k th analysis with information fraction t_k , the incremental error budget is $\Delta\alpha_k = \alpha^*(t_k) - \alpha^*(t_{k-1})$. The rejection boundaries $\{c_k\}$ are chosen so that, under H_0 and with respect to the limiting

Gaussian vector $(Z_1, \dots, Z_K)^\top$ in Corollary 4.4,

$$\mathbb{P}(Z_1 \geq c_1) = \Delta\alpha_1, \quad \mathbb{P}(Z_k \geq c_k, Z_j < c_j \text{ for all } j < k) = \Delta\alpha_k, \quad k = 2, \dots, K.$$

This construction ensures that $\mathbb{P}(\exists k \text{ such that } Z_k \geq c_k) = \alpha$. In the UNB design, the stopping rule is $\tilde{\tau} = \inf\{k \geq 1 : \Psi_{n_k} \geq c_k\}$, and H_0 is rejected if and only if $\tilde{\tau} \leq K$.

Algorithm 2 summarizes the sequential test procedure under UNB.

Algorithm 2 UNB allocation with information fraction group sequential test

Require: Significance level α , target power $1-\eta$, number of looks K , information fraction $t_j = j/K$, α spending function, budget $\{N_t\}$, burn in t_{\min} .

- 1: *Phase I: Design calibration*
 - 2: Compute \tilde{I}_{\max} and critical values $\{c_j\}_{j=1}^K$ under the α spending function and information fraction $\{t_j\}_{j=1}^K$.
 - 3: *Phase II: Initialization*
 - 4: Set $j \leftarrow 1$ and initialize the cumulative statistics.
 - 5: *Phase III: Adaptive allocation and sequential test*
 - 6: **for** $t = 1, 2, \dots$ **do**
 - 7: Draw $\mathbf{X}_t \sim \text{Multi-Hyper}(N_t; \mathbf{R}_{t-1})$ and set $\mathcal{A}_t = \{k : X_{t,k} > 0\}$. Observe $\boldsymbol{\xi}_t$, with $\xi_{t,k} = 0$ for $k \notin \mathcal{A}_t$. Update $\mathbf{R}_t \leftarrow \mathbf{R}_{t-1} + \mathbf{X}_t \odot \boldsymbol{\xi}_t$.
 - 8: *Update cumulative weighted sums*
 - 9: $W_{t,k} \leftarrow W_{t-1,k} + X_{t,k}$, $A_{t,k} \leftarrow A_{t-1,k} + X_{t,k}\xi_{t,k}$, $B_{t,k} \leftarrow B_{t-1,k} + X_{t,k}\xi_{t,k}^2$,
 - 10: $U_{t,ks} \leftarrow U_{t-1,ks} + X_{t,k}X_{t,s}$, $C_{t,ks} \leftarrow C_{t-1,ks} + X_{t,k}X_{t,s}\xi_{t,k}\xi_{t,s}$.
 - 11: *Update moment estimators as in Lemma A.3*
 - 12: $\hat{m}_{N,t} \leftarrow \frac{(t-1)\hat{m}_{N,t-1} + N_t}{t}$, $\hat{m}_{Q,t} \leftarrow \frac{(t-1)\hat{m}_{Q,t-1} + N_t^2}{t}$, $\hat{Z}_{k,t} \leftarrow \frac{(t-1)\hat{Z}_{k,t-1} + X_{t,k}/N_t}{t}$,
 - 13: $\hat{\mu}_{k,t} \leftarrow \frac{A_{t,k}}{W_{t,k}}$, $\hat{q}_{k,t} \leftarrow \frac{B_{t,k}}{W_{t,k}}$, $\hat{\sigma}_{k,t}^2 \leftarrow \hat{q}_{k,t} - \hat{\mu}_{k,t}^2$.
 - 14: For pairs $k \neq s$ with $U_{t,ks} > 0$, $\hat{q}_{ks,t} \leftarrow \frac{C_{t,ks}}{U_{t,ks}}$, $\hat{C}_{ks,t} \leftarrow \hat{q}_{ks,t} - \hat{\mu}_{k,t}\hat{\mu}_{s,t}$.
 - 15: *Plug-in variance estimation as in Theorem 3.2, (4) and (5)*
 - 16: Construct $\hat{\boldsymbol{\Sigma}}_t$ by (4). Set $\mathbf{b}_t = \left(\frac{\partial_1(h(\boldsymbol{\mu}))}{\sqrt{W_{t,1}}}, \dots, \frac{\partial_d(h(\boldsymbol{\mu}))}{\sqrt{W_{t,d}}}\right)^\top$, $\hat{\sigma}_{h,t}^2 \leftarrow \mathbf{b}_t^\top \hat{\boldsymbol{\Sigma}}_t \mathbf{b}_t$,
 - 17: $\Psi_t \leftarrow \frac{h(\hat{\boldsymbol{\mu}}_t)}{\hat{\sigma}_{h,t}}$. Set $I_t \leftarrow \frac{1}{\hat{\sigma}_{h,t}^2}$ and $t_t \leftarrow \frac{I_t}{I_{\max}}$
 - 18: *Boundary checks at interim looks*
 - 19: **while** $t \geq t_{\min}$ **and** $j \leq K$ **and** $t_t \geq t_j$ **do**
 - 20: **if** $\Psi_t > c_j$ **then**
 - 21: **return** Reject H_0 and stop.
 - 22: **end if**
 - 23: $j \leftarrow j + 1$
 - 24: **end while**
 - 25: **if** $I_t \geq I_{\max}$ **then**
 - 26: **return** Fail to reject H_0 and stop.
 - 27: **end if**
 - 28: **end for**
-

The spending function $\alpha^*(\cdot)$ determines the shape of efficacy boundaries over informa-

tion time. Choices include the Pocock-like, O’Brien–Fleming-like (OBF), power-type, and Hwang–Shih–DeCani (HS) families (Lan and DeMets, 1983):

$$\alpha_1^*(t) = \alpha \ln(1 + (e - 1)t), \quad \alpha_2^*(t) = 1 - \Phi\left(\frac{z_\alpha}{\sqrt{t}}\right), \quad \alpha_3^*(t) = \alpha t^q, \quad \alpha_4^*(t) = \alpha \frac{1 - e^{-\gamma t}}{1 - e^{-\gamma}}.$$

In Sections 5 and 6, we adopt an OBF-like spending function, which yields conservative early boundaries relative to the accumulated information fraction and ensures rigorous control of the overall Type I error under adaptive allocation.

5 Simulation Studies

This section presents a Monte Carlo study of the finite sample behavior of the proposed UNB based on the evaluation metrics Type I error control, power, and early stopping behavior compared with ER as a non-adaptive baseline and the UCB algorithm as a representative bandit baseline.

5.1 Fixed Sample Test

We first examine the fixed sample test performance in the two-arm comparison across Bernoulli, Poisson, and Exponential reward distributions. We evaluate empirical size under the binding null $H_0 : \mu_1 = \mu_2$ and empirical power at a representative alternative with $\mu_1 - \mu_2 = \Delta$ ($\Delta > 0$). In addition, we report the mean number of observations assigned to the inferior arm, S_{inf} , to quantify how each allocation rule trades off precision for reduced exposure to the inferior arm.

Under the independent cross-arm rewards scenario ($\rho = 0$), Table 4 (top panel) indicates that the UNB maintains empirical size close to the nominal level across all three reward distributions and achieves power close to the benchmark of ER. At the same total sample size, UNB allocates substantially more observations to the superior arm, yielding a marked decrease in mean S_{inf} . For instance, under the Bernoulli distribution, the mean S_{inf} drops from 115 (ER) to 79 with $(\mu_1, \mu_2) = (0.6, 0.4)$, and from 90 to 72 at $(0.8, 0.6)$. This pattern consistently holds for Poisson and Exponential outcomes, in-

dicating significantly reduced exposure to the inferior arm without material power loss. In the Bernoulli setting, UCB attains near-nominal size and power comparable to UNB and ER. By contrast, using the same two-sample studentized statistic with the standard normal critical value, UCB exhibits substantial size inflation in the Poisson and Exponential settings. One possible explanation is that the UCB index used here is calibrated via Hoeffding-type concentration, which is most natural for bounded or sub-Gaussian rewards and hence aligns well with Bernoulli outcomes. For Poisson and Exponential rewards, which are not sub-Gaussian, this calibration may be inadequate, potentially inducing overly aggressive concentration on one arm. The resulting severe imbalance and history dependence can invalidate the standard normal approximation, leading to inflated Type I error. When cross-arm rewards are correlated ($\rho = 0.5$), UNB maintains valid Type I error control while enabling adaptive allocation and early stopping, whereas ER and UCB exhibit inflated Type I error in the multi-draw setting, reflecting that their test statistics shown in Table 3 do not fully account for the covariance structure induced by cross-arm rewards and adaptive allocation.

5.2 Sequential Test

We next turn to the group sequential setting by employing the test procedure detailed in Algorithm 2 to allow for early stopping. Throughout, empirical size is evaluated under the null $H_0 : \mu_1 = \mu_2$ and simulations on checking statistical efficiency and ethical performance are conducted under alternatives $H_1 : \mu_1 - \mu_2 = \Delta$ ($\Delta > 0$) calibrated to a target power of $1 - \eta = 0.9$. For each type of reward distribution, we report empirical size, power, average sample number (ASN) used to attain the given power, alongside mean inferior arm exposure S_{inf} to quantify the ethics and statistical efficiency trade-off induced jointly by allocation and test.

Table 4 (bottom panel) summarizes these results. If cross arms are independent ($\rho = 0$), the simulated results imply UNB process maintains empirical size close to the nominal level and empirical power similar to the power benchmark ER across all scenarios under the target power 0.9. Meanwhile, UNB consistently reduces inferior arm

Table 4: Simulation results for fixed sample and sequential tests under Bernoulli, Poisson, and Exponential reward distributions with arm independent ($\rho = 0$) and correlated ($\rho = 0.5$, $N_n = 4$) settings are presented. Empirical size is evaluated under H_0 ; power, S_{inf} , and ASN (for sequential test only) are reported under H_1 , with sequential test calibrated to a target power of 0.9 across all considered scenarios. ER is the power benchmark in the fixed sample test. Notation “–” implies that results are omitted due to extreme Type I error inflation.

		Bernoulli												
(μ_1, μ_2, ρ)		S (0.6, 0.4, 0) 230			(0.8, 0.6, 0) 180			(0.6, 0.4, 0.5) 143			(0.8, 0.6, 0.5) 121			
		UNB	ER	UCB	UNB	ER	UCB	UNB	ER	UCB	UNB	ER	UCB	
Fixed Sample Test	Emp. Size	0.051	0.048	0.051	0.052	0.050	0.051	0.051	0.022	0.023	0.049	0.014	0.024	
	Emp. Power	0.909	0.919	0.898	0.901	0.914	0.897	0.912	–	–	0.909	–	–	
	Mean S_{inf}	79	115	55	72	90	46	64	–	–	57	–	–	
			Poisson											
	(μ_1, μ_2, ρ)		S (6.5, 6, 0) 840			(11, 10, 0) 380			(6.5, 6, 0.5) 527			(11, 10, 0.5) 225		
			UNB	ER	UCB	UNB	ER	UCB	UNB	ER	UCB	UNB	ER	UCB
		Emp. Size	0.048	0.048	0.106	0.049	0.049	0.086	0.052	0.019	0.025	0.051	0.020	0.031
		Emp. Power	0.900	0.899	–	0.898	0.914	–	0.896	–	–	0.896	–	–
		Mean S_{inf}	368	419	–	168	190	–	254	–	–	109	–	–
		Exponential												
(μ_1, μ_2, ρ)		S (7.5, 6, 0) 740			(12, 10, 0) 1140			(7.5, 6, 0.5) 425			(12, 10, 0.5) 674			
		UNB	ER	UCB	UNB	ER	UCB	UNB	ER	UCB	UNB	ER	UCB	
	Emp. Size	0.048	0.050	0.144	0.048	0.048	0.132	0.048	0.019	0.035	0.050	0.027	0.032	
	Emp. Power	0.908	0.907	–	0.907	0.932	–	0.891	–	–	0.900	–	–	
	Mean S_{inf}	264	370	–	413	570	–	190	–	–	304	–	–	
		Bernoulli												
(μ_1, μ_2, ρ)		(0.6, 0.4, 0)			(0.8, 0.6, 0)			(0.6, 0.4, 0.5)			(0.8, 0.6, 0.5)			
		UNB	ER	UCB	UNB	ER	UCB	UNB	ER	UCB	UNB	ER	UCB	
	Emp. Size	0.051	0.048	0.053	0.049	0.048	0.049	0.050	0.011	0.028	0.049	0.013	0.021	
	Emp. Power	0.917	0.900	0.906	0.912	0.890	0.879	0.917	–	–	0.901	–	–	
	ASN	160	156	195	138	132	188	274	–	–	229	–	–	
	Mean S_{inf}	61	78	50	58	66	47	91	–	–	88	–	–	
		Poisson												
(μ_1, μ_2, ρ)		(6.5, 6, 0)			(11, 10, 0)			(6.5, 6, 0.5)			(11, 10, 0.5)			
		UNB	ER	UCB	UNB	ER	UCB	UNB	ER	UCB	UNB	ER	UCB	
Sequential Test	Emp. Size	0.048	0.048	0.010	0.051	0.050	0.016	0.051	0.008	0.027	0.051	0.016	0.031	
	Emp. Power	0.906	0.894	–	0.908	0.892	–	0.853	–	–	0.742	–	–	
	ASN	648	631	–	265	262	–	1072	–	–	387	–	–	
	Mean S_{inf}	292	315	–	123	131	–	477	–	–	174	–	–	
		Exponential												
(μ_1, μ_2, ρ)		(7.5, 6, 0)			(12, 10, 0)			(7.5, 6, 0.5)			(12, 10, 0.5)			
		UNB	ER	UCB	UNB	ER	UCB	UNB	ER	UCB	UNB	ER	UCB	
	Emp. Size	0.052	0.050	0.033	0.048	0.050	0.012	0.052	0.011	0.065	0.049	0.009	0.060	
	Emp. Power	0.902	0.892	–	0.922	0.902	–	0.893	–	–	0.889	–	–	
	ASN	510	507	–	788	772	–	951	–	–	1435	–	–	
	Mean S_{inf}	195	254	–	297	386	–	338	–	–	531	–	–	

exposure S_{inf} , yielding more rewards than ER. For instance, in the Bernoulli setting with $(\mu_1, \mu_2) = (0.6, 0.4)$, UNB reduces mean S_{inf} from 78 (ER) to 61 while maintaining or even achieving slightly higher power; the same pattern holds for Poisson outcomes, where S_{inf} decreases from 315 to 292 at $(6.5, 6)$ and from 131 to 123 at $(11, 10)$, and for Exponential outcomes, where S_{inf} decreases from 254 to 195 at $(7.5, 6)$ and from 386 to 297 at $(12, 10)$. The corresponding ASNs under UNB are close to those under ER with smaller mean inferior arm exposure, suggesting that the exposure reductions are not necessarily obtained by materially increasing expected sample size, with differences $\mu_1 - \mu_2$ varying mildly by scenarios. The Bernoulli results for UCB additionally highlight the statistical efficiency cost of aggressive adaptation. While UCB attains comparable size and power, it yields a markedly larger ASN than UNB or ER (e.g., 195 vs. 160 or 156). On the other hand, the empirical size of UCB is not properly controlled under Poisson and Exponential outcomes and is omitted due to extreme Type I error inflation.

Table 4 (bottom panel) also demonstrates that the UNB based sequential test remains valid under cross-arm dependence, where multiple arms are sampled simultaneously and rewards are correlated. Across all scenarios with $\rho = 0.5$, the empirical size is well controlled around the nominal level. Under H_1 , the empirical power remains close to the target level 0.9, indicating that dependence does not distort the effective information accumulation required for sequential stopping. The larger ASN and increased inferior arm exposure S_{inf} are attributable to the simultaneous sampling protocol, reflecting the structural constraints of concurrent assignment. Since ER and UCB exhibit extreme Type I error inflation under fixed sample tests with cross-arm dependence, they are excluded from the sequential analysis in Table 4, which aims to support valid sequential inference in conjunction with adaptive allocation.

Figure 3 reports the ASN and S_{inf} across different Δ , which illustrates how early stopping and inferior arm exposure change as the difference of arms' expected reward increases. Under an information-based sequential design, for a given Δ , power is primarily driven by the accumulated information fraction and is thus approximately invariant across algorithm designs that admit asymptotically valid inference on the same information

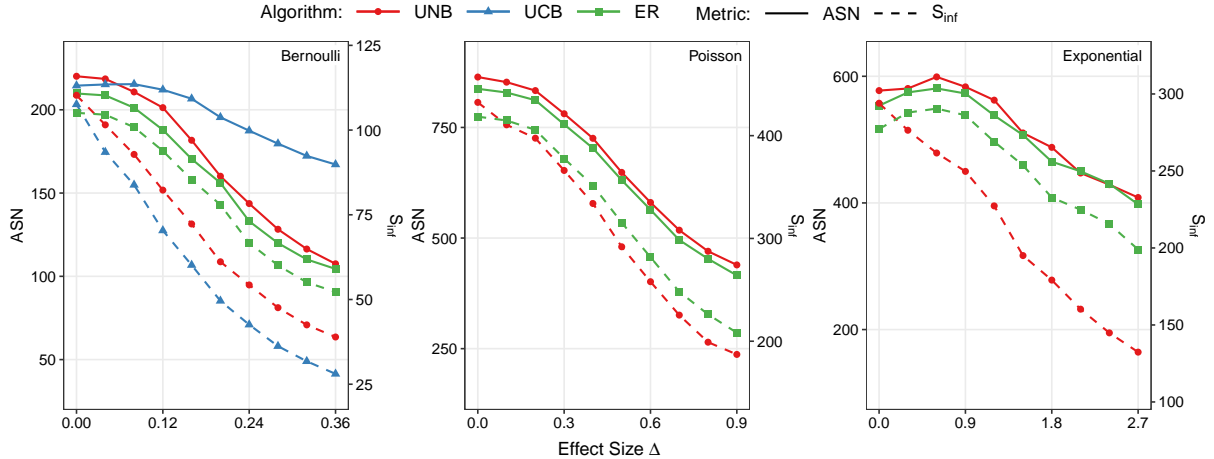


Figure 3: Dual-axis plots of ASN (left axis, solid lines) and S_{inf} (right axis, dashed lines) versus Δ for reward distributions under the information-based sequential design. UNB balance ethics and statistical efficiency in terms of the similar ASN to ER but smaller S_{inf} .

scale. Accordingly, we focus on ASN and S_{inf} as the primary metrics. The results imply that ASN decreases as the Δ increases, reflecting more frequent early boundary crossing under stronger signals; a mild nonmonotonicity for small difference of arms' expected reward can occur due to the discreteness of interim looks and early random imbalance in adaptive sampling. Meanwhile, S_{inf} also decreases with Δ , indicating that stronger effect sizes lead not only to earlier stopping but also to less relative allocation to the inferior arm. In all settings, UNB and ER yield similar ASN trajectories, while UNB consistently attains smaller S_{inf} , demonstrating ethical gains without a material increase in expected sample size. In the Bernoulli case, UCB produces the smallest inferior arm exposure proportion but at the cost of a larger ASN, consistent with the fact that extreme imbalance can slow information accumulation for two arm contrasts.

Ethics motivate allocating fewer observations to inferior arms, whereas inferential objectives favor allocations that preserve information for the target contrast (e.g., balanced sampling). This ethics-statistical efficiency tension is well recognized in response-adaptive and bandit-inspired trial designs; see, e.g., (Armitage, 1963; Villar et al., 2015). To summarize this trade-off on a single scale, we propose the weighted loss index:

$$L_{\lambda}(\mathcal{A}) = \text{ASN}(\mathcal{A}) + \lambda S_{\text{inf}}(\mathcal{A}), \quad (10)$$

where $\lambda > 0$ encodes the relative emphasis placed on reducing inferior arm exposure versus reducing expected sample size. In Figure 4, UNB matches or yields smaller weighted loss $L_\lambda(\mathcal{A})$ than ER and UCB across varying Δ for $\lambda \in \{2, 5\}$. Notably, the reduction in loss relative to ER is particularly pronounced under Exponential outcomes, reflecting a more effective trade-off between early stopping and inferior arm exposure. Baseline parameters under the null are $\mu_1 = \mu_2 = 0.6$ for Bernoulli, and $\mu_1 = \mu_2 = 10$ for both Poisson and Exponential outcomes.

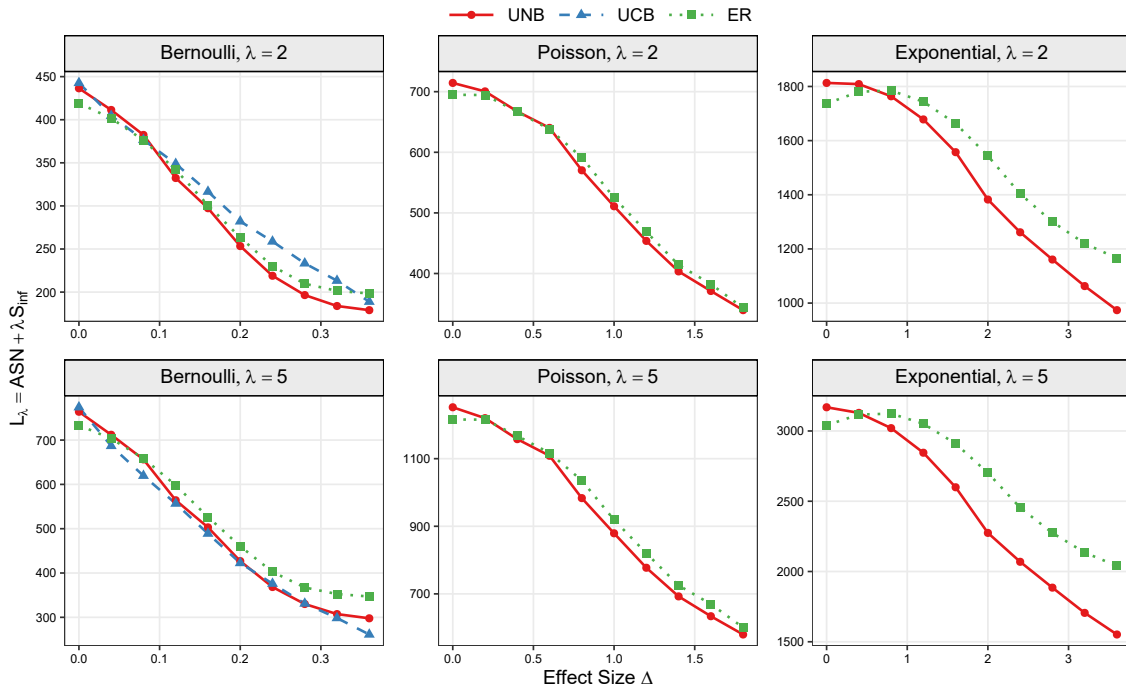


Figure 4: Loss index (10), $L_\lambda = \text{ASN} + \lambda S_{\text{inf}}$, as a function of Δ for different reward distributions under the information-based sequential design with $\lambda = 2$ (top) and $\lambda = 5$ (bottom). UNB performs better than ER and UCB with the increase of Δ .

6 Real Data Analysis

This section evaluates the performance of our method by using a real dataset referred to Dataset A from a world-leading ride-sharing company (anonymized for privacy). The data are collected through a randomized controlled trial in which users are randomly assigned to two different marketing strategies. To optimize economic returns, the company aims to evaluate strategy performance while prioritizing better-performing treatments and enabling early stopping once sufficient evidence is observed. Therefore, we formulate this

as a sequential test problem: $H_0 : \mu_1 = \mu_2$ versus $H_1 : \mu_1 - \mu_2 = \Delta > 0$.

Given the complexity and heterogeneity of real data and the generally unknown treatment effects, purely observational datasets do not allow rigorous evaluation of statistical methods. To address this, we construct a semi-synthetic dataset based on Dataset A by injecting controlled treatment effects into the observed data (Kohavi et al., 2020). This design enables rigorous assessment of Type I error, statistical power, and other performance metrics.

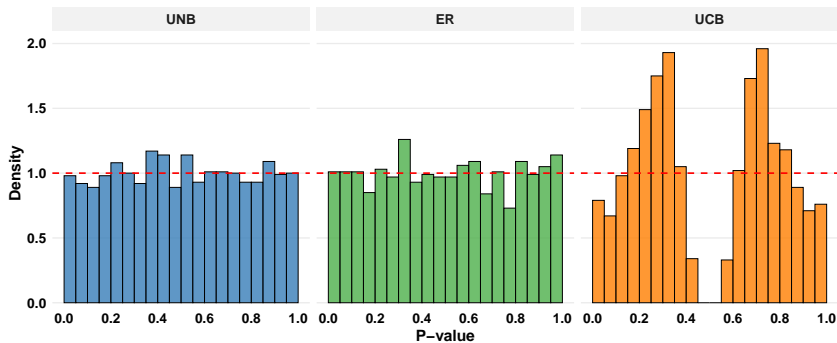


Figure 5: Empirical probability density of p -values under H_0 based on 2000 Monte Carlo samplings on the semi-synthetic real dataset. The red dashed line denotes the uniform distribution $U[0, 1]$. Like benchmark ER, UNB shows valid Type I error.

Figure 5 shows that UNB and ER produce approximately uniform p -values under H_0 , consistent with valid Type I error control, whilst UCB suffers extremely large Type I error inflation, reflecting adaptivity-induced selection bias that compromises the validity of standard inference. Consequently, UCB is omitted from the following performance evaluation on statistical power and average reward lift.

Figure 6 (left panel) evaluates test performance in a fixed sample setting. UNB attains competitive statistical power relative to the ER benchmark that maximizes power while substantially improving statistical efficiency by reducing inferior arm allocation (e.g., to 0.28 at $\Delta = 30\%$), yielding a 20.24% reward lift relative to the base reward level (prior to effect injection). In the sequential test framework, we adopt the policy that if the null hypothesis is rejected at an interim analysis, all remaining units are subsequently assigned to the treatment estimated to be superior. Specifically, for each difference of arms' expected reward, the reward lift is calculated over a horizon defined by the maximum average sample size required by the two algorithms (UNB and ER). The empirical results

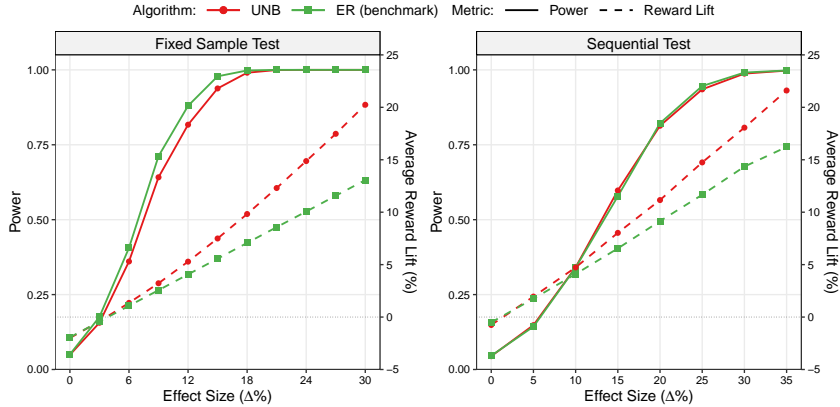


Figure 6: Performance comparison of allocation strategies under fixed sample test (left) and sequential test (right) frameworks. Solid lines (left y-axis) represent power of the test, while dashed lines (right y-axis) indicate the average reward lift (%). UNB attains the benchmark power of ER but improves larger average reward lift. UCB is deleted due to extremely large inflation of Type I error.

(Figure 6, right panel, and Table 5) suggest that both UNB and ER generally terminate early, and UNB systematically outperforms ER due to its adaptive allocation during the trial, achieving higher average reward lifts (e.g., 11.16% vs. 9.15% at a 20% difference of arms’ expected reward, 18.06% vs. 14.35% at a 30% difference of arms’ expected reward). This demonstrates that UNB yields a more favorable balance between statistical efficiency and overall reward.

Table 5: Sequential test performance on the semi-synthetic dataset. Results include ASN, ASS, and average reward lift are reported under relative effect sizes of 10%, 20% and 30%. A design effect size of 20% achieves 0.80 power and $K = 10$.

Scenario	ASN		ASS		Avg. Lift(%)	
	UNB	ER	UNB	ER	UNB	ER
H_0	2748	2653	9.89	9.89	-0.76	-0.51
H_1 (10%)	2469	2417	9.14	9.18	4.73	3.98
H_1 (20%)	1949	1955	7.24	7.37	11.16	9.15
H_1 (30%)	1480	1412	5.39	5.47	18.06	14.35

7 discussion

This work advances the integration of adaptive allocation and sequential test in experimental design and significantly improves the statistical efficiency and ethicality of adaptive designs by dynamically prioritizing better performing treatments. Theoretical

results overcome the limitations of traditional methods, which often assume independent and sub-Gaussian observations and focus solely on cumulative regret, thus enabling precise confidence intervals and hypothesis testing in complex scenarios. Further studies can focus on highly dynamic environments with nonstationary reward distributions, such as online recommendation systems with evolving user preferences. Computational complexity may pose challenges in large-scale applications with many arms.

Supplementary Material

Detailed proofs of all theoretical results and an additional real-data analysis table are deferred to the Supplementary Material.

A Auxiliary Lemmas

This section collects several key asymptotic properties of the UNB allocation process, which are foundational to our main results. Proofs of these lemmas are provided in [Yang et al. \(2024\)](#).

Lemma A.1. *Suppose Assumptions 1–2 hold. Under the UNB processes, we have*

$$\frac{\sum_{i=1}^d R_{n,i} \mathbb{I}(\mu_i = \mu^*)}{|\mathbf{R}_n|} \xrightarrow{a.s.} 1, \quad \frac{\sum_{i=1}^d W_{n,i} \mathbb{I}(\mu_i = \mu^*)}{|\mathbf{W}_n|} \xrightarrow{a.s.} 1, \quad \text{and} \quad \frac{\mathbf{R}_n}{|\mathbf{R}_n|} \xrightarrow{a.s.} \mathbf{Z},$$

where the limiting components satisfy $Z_k = 0$ if $\mu_k < \mu^*$, and $Z_k \in (0, 1]$ otherwise.

Lemma A.2. *Suppose Assumptions 1–2 hold. For each arm $k \in \{1, 2, \dots, d\}$, the normalized allocation $\frac{W_{n,k}}{n^{\mu_k/\mu^*}}$ converges almost surely to a random variable \tilde{Z}_k satisfying $\mathbb{P}(0 < \tilde{Z}_k < \infty) = 1$.*

Lemma A.3. *Suppose Assumptions 1–2 hold. Define that*

$$q_{k,n} = \mathbb{E}(\xi_{n,k}^2) \rightarrow q_k, \quad q_{ks,n} = \mathbb{E}(\xi_{n,k} \xi_{n,s}) \rightarrow q_{ks}.$$

Then for all $k, s \in \{1, \dots, d\}$, the following hold almost surely:

1. *Sample Moments of N_j* : $\frac{1}{n} \sum_{j=1}^n N_j \rightarrow N$ and $\frac{1}{n} \sum_{j=1}^n N_j^2 \rightarrow Q$.
2. *Reward Proportions*: $\hat{Z}_{k,n} = \frac{1}{n} \sum_{j=1}^n X_{j,k}/N_j \rightarrow Z_k$.
3. *Mean and Moment Estimators*: The estimators

$$\hat{\mu}_{k,n} = \frac{\sum_{j=1}^n \xi_{j,k} X_{j,k}}{W_{n,k}}, \quad \hat{q}_{k,n} = \frac{\sum_{j=1}^n \xi_{j,k}^2 X_{j,k}}{W_{n,k}}, \quad \text{and} \quad \hat{q}_{ks,n} = \frac{\sum_{j=1}^n \xi_{j,k} \xi_{j,s} X_{j,k} X_{j,s}}{\sum_{j=1}^n X_{j,k} X_{j,s}}$$

converge to μ_k, q_k , and q_{ks} (for $k \neq s$ and $N > 1$), respectively.

Note that based on the estimators of the second-order and cross moments of the random variable sequence $\{\xi_{n,k}\}$ provided in Lemma A.3, the estimators of the cross-arm covariance and correlation coefficients are given by

$$\hat{C}_{ks,n} = \hat{q}_{ks,n} - \hat{\mu}_{k,n} \hat{\mu}_{s,n}, \quad \text{and} \quad \hat{\rho}_{ks,n} = \hat{C}_{ks,n} / \sqrt{\hat{q}_{k,n} \hat{q}_{s,n}}.$$

References

- R. Agrawal. Sample mean based index policies with $o(\log n)$ regret for the multi-armed bandit problem. *Advances in Applied Probability*, 27:1054–1078, 1995.
- S. Agrawal and N. Goyal. Analysis of thompson sampling for the multi-armed bandit problem. In *Proceedings of the 25th Annual Conference on Learning Theory*, volume 23, pages 39.1–39.26. PMLR, 2012.
- V. Anantharam, P. Varaiya, and J. Walrand. Asymptotically efficient allocation rules for the multiarmed bandit problem with multiple plays—Part I: I.I.D. rewards. *IEEE Transactions on Automatic Control*, 32(11):968–976, 1987.
- P. Armitage. *Sequential Medical Trials*. Blackwell Scientific Publications, Oxford, 1960.
- P. Armitage. Sequential medical trials: Some comments on F. J. Anscombe’s paper. *Journal of the American Statistical Association*, 58(302):384–387, 1963.

- P. Armitage, C. K. McPherson, and B. C. Rowe. Repeated significance tests on accumulating data. *Journal of the Royal Statistical Society, Series A*, 132(2):235–244, 1969.
- J. Y. Audibert, R. Munos, and C. Szepesvári. Exploration–exploitation tradeoff using variance estimates in multi-armed bandits. *Theoretical Computer Science*, 410(19):1876–1902, 2009.
- P. Auer, N. Cesa-Bianchi, and P. Fischer. Finite-time analysis of the multiarmed bandit problem. *Machine Learning*, 47:235–256, 2002.
- Y. Chen and J. Lu. A characterization of sample adaptivity in UCB data. *arXiv preprint arXiv:2503.04855*, 2025.
- D. S. Gaharwar, I. Juneja, D. Varshney, and S. Moharir. A new approach to correlated multi-armed bandits. In *2020 12th International Conference on Communication Systems & Networks*, pages 634–637, 2020.
- B. Gang, W. Sun, and W. Wang. Structure-adaptive sequential testing for online false discovery rate control. *Journal of the American Statistical Association*, 118(541):732–745, 2021.
- A. Garivier and O. Cappé. The KL-UCB algorithm for bounded stochastic bandits and beyond. In *Proceedings of the 24th Annual Conference on Learning Theory*, volume 19 of *Proceedings of Machine Learning Research*, pages 359–376. PMLR, 2011.
- S. Gupta, S. Chaudhari, G. Joshi, and O. Yağan. Multi-armed bandits with correlated arms. *IEEE Transactions on Information Theory*, 67(10):6711–6732, 2021.
- P. Hall and C. C. Heyde. *Martingale Limit Theory and Its Applications*. Academic Press, New York, 1980.
- F. Hu and W. F. Rosenberger. *The Theory of Response-Adaptive Randomization in Clinical Trials*. John Wiley & Sons, Hoboken, NJ, 2006.

- C. Jennison and B. W. Turnbull. *Group Sequential Methods with Applications to Clinical Trials*. Chapman and Hall/CRC, Boca Raton, FL, 2000.
- R. Johari, P. Koomen, L. Pekelis, and D. Walsh. Peeking at A/B tests: Why it matters, and what to do about it. In *Proceedings of the 23rd ACM SIGKDD International Conference on Knowledge Discovery and Data Mining*, pages 1517–1525, 2017.
- R. Johari, P. Koomen, L. Pekelis, and D. Walsh. Always valid inference: Continuous monitoring of A/B tests. *Operations Research*, 70(3):1806–1821, 2022.
- N. Ju, D. Hu, A. Henderson, and L. Hong. A sequential test for selecting the better variant: Online A/B testing, adaptive allocation, and continuous monitoring. In *Proceedings of the Twelfth ACM International Conference on Web Search and Data Mining*, pages 492–500, 2019.
- M. Kano, J. Honda, K. Sakamaki, K. Matsuura, A. Nakamura, and M. Sugiyama. Good arm identification via bandit feedback. *Machine Learning*, 108(5):721–745, 2019.
- K. Khamaru and C. Zhang. Inference with the upper confidence bound algorithm. *arXiv preprint arXiv:2408.04595*, 2024.
- R. Kohavi, D. Tang, and Y. Xu. *Trustworthy Online Controlled Experiments: A Practical Guide to A/B Testing*. Cambridge University Press, 2020.
- T. L. Lai and H. Robbins. Asymptotically efficient adaptive allocation rules. *Advances in Applied Mathematics*, 6:4–22, 1985.
- K. K. G. Lan and D. L. DeMets. Discrete sequential boundaries for clinical trials. *Biometrika*, 70(3):659–663, 1983.
- K. K. G. Lan and D. M. Zucker. Sequential monitoring of clinical trials: The role of information and brownian motion. *Statistics in Medicine*, 12:753–765, 1993.
- K. K. G. Lan, D. M. Reboussin, and D. L. DeMets. Information and information fractions for design and sequential monitoring of clinical trials. *Communications in Statistics-Theory and Methods*, 23(2):403–420, 1994.

- N. Larsen, J. Stallrich, S. Sengupta, A. Deng, R. Kohavi, and N. T. Stevens. Statistical challenges in online controlled experiments: A review of A/B testing methodology. *The American Statistician*, 78(2):135–149, 2024.
- A. Locatelli, M. Gutzeit, and A. Carpentier. An optimal algorithm for the thresholding bandit problem. In *Proceedings of the 33rd International Conference on Machine Learning*, volume 48, pages 1690–1698. PMLR, 2016.
- O.-A. Maillard and R. Munos. Adaptive bandits: Towards the best history-dependent strategy. In *Proceedings of the Fourteenth International Conference on Artificial Intelligence and Statistics*, volume 15, pages 570–578. PMLR, 2011.
- C. May and N. Flournoy. Asymptotics in response-adaptive designs generated by a two-color, randomly reinforced urn. *The Annals of Statistics*, 37(2):1058–1078, 2009.
- X. Nie, X. Tian, J. Taylor, and J. Zou. Why adaptively collected data have negative bias and how to correct for it. In *Proceedings of the 21st International Conference on Artificial Intelligence and Statistics*, volume 84, pages 1261–1269. PMLR, 2018.
- P. C. O’Brien and T. R. Fleming. A multiple testing procedure for clinical trials. *Biometrics*, 35(3):549–556, 1979.
- S. J. Pocock. Group sequential methods in the design and analysis of clinical trials. *Biometrika*, 64(2):191–199, 1977.
- M. A. Proschan, K. K. G. Lan, and J. T. Wittes. *Statistical Monitoring of Clinical Trials: A Unified Approach*. Springer, New York, NY, 2006.
- M. A. Proschan, M. Nason, A. M. Ortega-Villa, and J. Wang. Changing interim monitoring in response to internal clinical trial data. *Biometrics*, 80(1):ujae006, 2024.
- H. Qi, F. Guo, and L. Zhu. Thompson sampling for non-stationary bandit problems. *Entropy*, 27(1):51, 2025.
- A. Ramdas, P. Grünwald, V. Vovk, and G. Shafer. Game-theoretic statistics and safe anytime-valid inference. *Statistical Science*, 38(4):576–601, 2023.

- A. Rényi. On stable sequences of events. *Sankhyā: The Indian Journal of Statistics, Series A*, 25(3):293–302, 1963.
- W. F. Rosenberger and J. M. Lachin. *Randomization in Clinical Trials: Theory and Practice*. John Wiley & Sons, Hoboken, NJ, 2nd edition, 2016.
- C. Shi, S. Luo, H. Zhu, and R. Song. An online sequential test for qualitative treatment effects. *Journal of Machine Learning Research*, 22:1–51, 2021.
- C. Shi, R. Wan, G. Song, S. Luo, H. Zhu, and R. Song. A multi-agent reinforcement learning framework for off-policy evaluation in two-sided markets. *The Annals of Statistics*, 51(6):2455–2480, 2023.
- R. S. Sutton and A. G. Barto. *Reinforcement Learning: An Introduction*. MIT Press, Cambridge, MA, 2nd edition, 2018.
- B. Thananjeyan, K. Kandasamy, I. Stoica, M. I. Jordan, K. Goldberg, and J. E. Gonzalez. Resource allocation in multi-armed bandit exploration: Overcoming sublinear scaling with adaptive parallelism. In *International Conference on Machine Learning*, volume 139, pages 10236–10246. PMLR, 2021.
- W. R. Thompson. On the likelihood that one unknown probability exceeds another in view of the evidence of two samples. *Biometrika*, 25(3–4):285–294, 1933.
- S. Villar, J. Bowden, and J. Wason. Multi-armed bandit models for the optimal design of clinical trials: benefits and challenges. *Statistical Science*, 30(2):199–215, 2015.
- A. Wald. Sequential tests of statistical hypotheses. *The Annals of Mathematical Statistics*, 16(2):117–186, 1945.
- J. Wang, C. Shi, and Z. Wu. A robust test for the stationarity assumption in sequential decision making. In *Proceedings of the 40th International Conference on Machine Learning*, volume 202, pages 36355–36379. PMLR, 2023.

- W. Wang, B. Gang, and W. Sun. Sparse recovery with multiple data streams: An adaptive sequential testing approach. *Journal of Machine Learning Research*, 25:1–59, 2024.
- I. Waudby-Smith, L. Wu, A. Ramdas, N. Karampatziakis, and P. Mineiro. Anytime-valid off-policy inference for contextual bandits. *ACM/IMS Journal of Data Science*, 1(3): 1–42, 2024.
- L. J. Wei and S. Durham. The randomized play-the-winner rule in medical trials. *Journal of the American Statistical Association*, 73(364):840–843, 1978.
- Y. Xia, T. Qin, W. Ma, N. Yu, and T.-Y. Liu. Budgeted multi-armed bandits with multiple plays. In *Proceedings of the 25th International Joint Conference on Artificial Intelligence*, pages 2210–2216. AAAI Press, 2016.
- L. Yang, J. Hu, J. Li, and Z. Bai. Asymptotic properties of a multicolored random reinforced urn model with an application to multi-armed bandits. *arXiv preprint arXiv:2406.10854*, 2024.
- S. Yu, S. Fang, R. Peng, Z. Qi, F. Zhou, and C. Shi. Two-way deconfounder for off-policy evaluation in causal reinforcement learning. In *Advances in Neural Information Processing Systems*, volume 37, 2024.
- Y. Zhang, S. Zhao, B. Wan, J. Wang, and X. Yan. Strategic A/B testing via maximum probability-driven two-armed bandit. In *Proceedings of the 42nd International Conference on Machine Learning*, volume 267, pages 77069–77089. PMLR, 2025.
- H. Zhu and F. Hu. Sequential monitoring of response-adaptive randomized clinical trials. *The Annals of Statistics*, 38(4):2218–2241, 2010.
- H. Zhu and F. Hu. Interim analysis of clinical trials based on urn models. *The Canadian Journal of Statistics*, 40(3):550–568, 2012.